Research Square

Preprints are preliminary reports that have not undergone peer review.
They should not be considered conclusive, used to inform clinical practice,
or referenced by the media as validated information.

# Low flow enhances pigmentation and lipid reserves but reduces survival in newly settled Acropora digitifera corals

**Saskia Jurriaans**

s.jurriaans@aims.gov.au

Australian Institute of Marine Science

**Mark Deleja**

Australian Institute of Marine Science

**Victoria Jenkins**

Australian Institute of Marine Science

**Annika Withers**

AIMS@JCU, James Cook University

**Carrie A. Sims**

Smithsonian Tropical Research Institute

**Carly J. Randall**

Australian Institute of Marine Science

**Research Article**

**Keywords:** Hydrodynamics, early life stage, coral aquaculture, reef restoration, energy allocation, symbiont acquisition

**Posted Date:** June 28th, 2026

**DOI:** https://doi.org/10.21203/rs.3.rs-9963159/v1

**License:** This work is licensed under a Creative Commons Attribution 4.0 International License.
Read Full License

**Additional Declarations:** No competing interests reported.

# Abstract

Water flow is a key driver of coral performance, yet its effects on newly settled corals (hereafter spat) remain poorly understood. Here we show that flow effects on *Acropora digitifera* spat are response-specific and time-dependent. We tested how flow influences survival, symbiont acquisition, and lipid content and composition in *A. digitifera* spat for 83 days following settlement. Spat were reared under low (0.01 m $s^{-1}$), moderate (0.05 m $s^{-1}$), and high (0.15 m $s^{-1}$) flow regimes, with a continuous supply of symbiont cells provisioned for the first six days post-settlement. Spat survival was assessed through weekly imaging, pigmentation was scored using a four-point visual scale as a proxy for symbiont acquisition, and total lipid content and lipid-class composition were measured through time. Survival differed among flow regimes, with early mortality risk under low flow 6.1-fold and 21.7-fold higher than under moderate and high flow, respectively. In contrast, low-flow spat developed higher pigmentation scores and had greater total lipid content than those under moderate or high flow. Lipid-class composition changed through time but showed little response to flow. Flow conditions associated with rapid symbiont acquisition and larger lipid reserves did not maximise early survival for *A. digitifera* spat, highlighting the need to assess multiple measures of spat performance across longer timeframes and broader experimental contexts.


# Introduction

Coral reefs are under increasing pressure due to climate change and local stressors, with repeated mass bleaching events impacting adult coral cover (Emslie et al. 2025; Eakin et al. 2026) and reproductive output (Hughes et al. 2019; Briggs et al. 2024). Population recovery depends on the successful settlement and survival of newly settled corals (hereafter spat), which add new individuals to populations already under stress. However, the post-settlement period is characterised by very high mortality, particularly during the first months after settlement but often continuing through the juvenile stage (Jurriaans et al. 2025; Smith et al. 2025), making it a major demographic bottleneck (Edmunds 2023). During this period, spat are exposed to multiple biotic pressures, such as predation, incidental grazing, and benthic competition (Trapon et al. 2013; Doropoulos et al. 2016). In addition, abiotic environmental conditions such as light availability, temperature, water flow, nutrient concentrations, and sedimentation can strongly influence physiological performance and spat survival (Humanes et al. 2017; Hancock et al. 2021). This bottleneck is also relevant to coral aquaculture and restoration, where sexually propagated corals are increasingly used to improve genetic diversity and scale coral seeding efforts, but where post-settlement survival remains a major constraint (Randall et al. 2020). Identifying the environmental conditions that support spat performance is therefore important for both natural recovery processes and restoration practice.

Among these environmental factors, water flow has long been recognized as critical in structuring coral communities (e.g., Jokiel 1978; Jokiel and Morrissey 1993; Madin et al. 2006; Nakamura 2010). Flow supports nutrient uptake, growth and recovery, which has been particularly evident after bleaching (Nakamura and Van Woesik 2001; Lentz et al. 2024). Increased flow enhances the diffusion of

metabolites (i.e. mass transfer) and heat across the coral boundary layer, reducing oxidative stress and enhancing photosynthesis and nitrogen fixation (Finelli et al. 2006; Nakamura 2010). Flow also promotes calcification (Dennison and Barnes 1988; Atkinson and Bilger 1992), facilitates sediment removal (Duckworth et al. 2017), and influences symbiont uptake, larval dispersal and settlement processes (Reidenbach et al. 2009; Eagle et al. 2012; Gouezo et al. 2025). Taken together, water flow is consequential for all coral life stages, including early survival and growth.

While the effects of flow on adult colonies are well documented, less is known about the mechanisms by which flow influences the early life stages of corals. Spat differ from adults in their morphology, size (i.e., surface area to volume ratios), and boundary-layer dynamics, and they face distinctly different physiological demands, meaning that their interactions with flow cannot necessarily be inferred from adult colonies (Edmunds 2023). Following spawning and fertilization, coral larvae must attach to the substrate and metamorphose, then initiate calcification and begin building a skeleton, all of which impose high energetic demands. For example, respiration in newly settled *Seriatopora caliendrum* spat increased rapidly during the first few days after settlement, suggesting that early post-settlement development is supported by substantial metabolic investment and the use of internal energy reserves (Edmunds et al. 2013). Additionally, many broadcast-spawning corals, including *Acropora*, acquire symbionts horizontally from the environment during larval or juvenile stages (Baird et al. 2009). Establishing symbiosis is a key developmental transition because symbionts provide photosynthetically derived energy during early growth, and early symbiont acquisition has been shown to enhance post-settlement survival in *Acropora* (Suzuki et al. 2013). During this energetically demanding transition period, lipid reserves may serve as a major energy source, supporting metabolism until symbiosis is fully established (Edmunds et al. 2013). The lipid composition of spat can change substantially throughout development, settlement, and post-settlement ontogeny (Figueiredo et al. 2012; Roper et al. 2024). Together, symbiont uptake and lipid reserves provide complementary insights into the physiological status of coral spat, potentially revealing responses to environmental conditions that survival alone does not capture.

It remains unclear how survival, symbiont acquisition, and energy reserves interact in coral spat, and how these relationships are influenced by water flow. Examining these response variables together is therefore critical for identifying the mechanisms through which flow shapes spat performance. Here we tested how three flow regimes influenced the early performance of *Acropora digitifera* spat by quantifying survival, visual pigmentation scores as a proxy for symbiont cell density, and lipids through time. Specifically, we asked whether flow regime affected (1) survival trajectories, (2) the rate and extent of pigmentation development, (3) total lipid content, and (4) lipid-class composition during early development.

## Methods

# Coral collection, spawning, rearing and settlement

Fifteen gravid *Acropora digitifera* colonies were collected from Moore Reef in early February 2022 (permit G21/45348.1, Reef Authority, Australia) and transported by boat to the National Sea Simulator (SeaSim) at the Australian Institute of Marine Science (AIMS, Townsville, Australia). Colonies were maintained in outdoor flow-through tanks under reef-specific temperature and natural light. The full moon on 17 February 2022 marked the autumn spawning period for this species. Colonies were monitored nightly thereafter, with spawning occurring 11 days post-full moon. Gamete bundles were collected from five colonies and cross-fertilised to produce larval cultures, which were reared following Pollock et al. (2017). Settlement competency was first observed six days post-spawning through standard settlement assays (Heyward and Negri 1999). Larvae were settled on two pre-conditioned concrete settlement tiles (conditioned for six weeks in flow-through seawater). Each tile (280 x 280 mm) was made from a 9:2 concrete-to-mortar mix (Dingo Cement Pty Ltd, Australia) and comprised 400 individual settlement Tables (14 x 14 mm each; see Ramsby et al. 2025 for details). Two days after settlement, tiles were cut into individual tabs using a blunt slicer submerged in seawater. Tabs with spat were inspected under magnification to count colonies and tabs were grouped by spat density: 5 spat per tab (n = 24 tabs), 6–10 spat per tab (n = 159 tabs) and 11–15 spat per tab (n = 42 tabs). Tabs were then glued onto PVC strips (15 tabs per strip; ~240 x 20 mm), ensuring that each strip contained the same total number of spat (~ 100) while the position of density groups was randomized. Spat were held in flow-through 4 µm-filtered seawater at reef-specific temperature under low light (~ 50 µmol photons $m^{-2}$ $s^{-1}$ 12 h light:12 h dark cycle) until the start of the experiment, nine days post-settlement.

## Experimental design and flow treatments

Three flow regimes were used: low (0.01 m $s^{-1}$), moderate (0.05 m $s^{-1}$), and high (0.15 m $s^{-1}$; Fig. 1a). The velocities were selected to span ecologically relevant hydrodynamic conditions experienced by coral spat. The low and moderate treatments were chosen to be comparable to flow conditions reported from coral recruitment habitats at One Tree Reef (~ 0.02–0.07 m $s^{-1}$; Eagle et al. 2012), whereas the high flow regime falls within cross-reef flows reported for reef-lagoon systems (0.10–0.20 m $s^{-1}$; Lowe et al. 2009) and nursery environments (< 0.50 m $s^{-1}$; Lentz et al. 2024). This range also overlaps with flow regimes tested for prey capture in newly settled corals (0-0.20 m $s^{-1}$; Geertsma et al. 2022). Low-flow conditions are biologically relevant because small spat interact with seawater differently than larger colonies, and respiration can become mass-transfer limited at low flow speeds and low Reynolds (*Re*) numbers ( i.e., the ratio of inertial forces to viscous forces, which influences whether flow is laminar (low *Re*) or turbulent (high *Re*); Edmunds 2023).

Each flow regime was generated in a separate, computer-controlled flume tank that was designed, built, and tested at AIMS, and described by Illing et al. (2021). Briefly, each flume contained five parallel raceways (244 mm in length) with rounded bases and extended flow straighteners that produced highly uniform, rectilinear flow. Flow was driven by a recirculating pump system connected to a large sump (~ 2400 L) and regulated automatically via programmable logic control to maintain steady velocities with minimal turbulence. The three flume systems were connected via an overflow between sumps, ensuring

a shared water supply and similar water conditions across the three flow regimes. Within each flume, the five raceways served as technical replicates, and each held one PVC strip containing 15 settlement tabs. Flow within the raceways was continuous and spatially homogeneous (Illing et al. 2021), ensuring that spat within each flow treatment experienced comparable hydrodynamic conditions.

## Symbiont inoculation and dosing validation

Symbiont inoculations were conducted using a *Cladocopium goreaui* strain SCF055-01.10 from the AIMS Symbiont Culture Facility. Symbiont densities in the stock culture were determined from five replicate 5 ml subsamples, each counted in quadruplicate using a haemocytometer. Inoculations began at the start of the experiment and were delivered continuously for six days (Fig. 1c) via a dosing cone connected to a peristaltic pump (ISMATEC IPC, Ismatec SA, Switzerland). The system was calibrated to maintain a constant flow rate of 10 ml $min^{-1}$ per flume for 17 h $day^{-1}$, corresponding to a target concentration of approximately 150 cells $ml^{-1}$ across all flow regimes. This concentration was selected to provide a low, sustained supply of symbionts, approximating the environmental source pools from which juvenile *Acropora* acquire symbionts during early symbiosis establishment (Quigley et al. 2017). Each flume's dosing cone received a daily mixture of symbiont culture diluted to 10 l with 4 µm-filtered seawater. The volume of symbiont culture added to each dosing cone was adjusted according to the flow regime, with 70 ml, 351 ml, and 1053 ml added for the low, moderate, and high flow regime, respectively, to maintain comparable target concentrations in the flumes.

To validate the dosing method and assess symbiont suspension in the circulating system, water samples were collected during the first two weeks of the experiment (Fig. 1c). For each flow regime, triplicate 800 ml water samples were collected from the outlet of each flume at 7 time points (3 flumes × 3 replicates × 7 time points; n = 63). In addition, to verify delivery concentrations, triplicate 10 ml samples were collected directly from the peristaltic pump outlet at the start and end of dosing on four sampling days (3 flumes × 3 replicates × 2 sampling times × 4 days; n = 72). Samples were preserved in 10% formalin. Symbiont cell concentrations were quantified by flow cytometry (Accuri C6, BD Biosciences) for flume outlet samples and by haemocytometry using a Neubauer improved haemocytometer for pump outlet samples, as the latter were too dense for cytometric counting. Replicate counts were averaged and converted to cell concentrations (cells $ml^{-1}$).

## Response variables: survival, pigmentation and lipid sampling

*Spat survival* - High-resolution images of submerged settlement tabs were taken at each census using a Nikon DSLR D810 camera and four Ikelite DS161 strobes connected to a computer-controlled camera system. Camera settings, strobe position, image distance, and lighting conditions were standardised across censuses to minimise variation in image colour and brightness unrelated to spat condition. From these images, survival and mortality were quantified. Survival was defined as the presence of intact living tissue. Spat were counted as either individuals or aggregates, with aggregates defined as two or

more adjacent spat in physical contact. Units were assigned at the first census and followed consistently through time.

*Spat pigmentation score* - Spat pigmentation was assessed from the same images used for survival tracking, using a four-point ordinal scale representing increasing visible pigmentation as a proxy for symbiont acquisition and relative symbiont density. This approach was based on previous work showing that colour variation in early coral life stages reflects differences in symbiont density (Chamberland et al. 2017), that coral colour scores can correspond to symbiont density and chlorophyll *a* content (Siebeck et al. 2006), and that image-derived colour metrics can provide quantitative proxies for Symbiodiniaceae density and chlorophyll content under standardised imaging conditions (Ferrara et al. 2026). Because scores were assigned from images collected under standardised imaging conditions, relative differences in visible pigmentation were interpreted as reflecting differences in symbiont acquisition and/or density, rather than differences in image exposure or illumination. Attempts to quantify symbiont uptake or photosynthetic performance using imaging PAM were unsuccessful because fluorescence from the surrounding substrate interfered with measurements of individual spat. Tissue samples also could not be used to quantify symbiont density because all available spat material was required for lipid analyses. Scores were therefore assigned as follows: 0 = no visible pigmentation, 1 = low pigmentation with sparse symbionts, 2 = intermediate pigmentation with distinguishable cells, and 3 = high pigmentation with dense, dark tissue, particularly in the tentacles (Fig. 1b, Supplementary Methods S1; Figure S1). To minimise scoring bias, all images were blinded before analysis by removing identifying information, including tab position, treatment, and census time. Scoring was performed by a trained reviewer in ImageJ software (version 1.54i, later upgraded to 1.54m; Schneider et al. 2012) following a standard operating procedure. To reduce the risk of shifting baseline bias, scoring consistency was maintained through regular calibration checks, and borderline cases were discussed against the scoring criteria before classification. Spat that were out of focus, obscured, broken, or otherwise could not be scored reliably were excluded from analysis.

*Lipid sampling* - Tabs were destructively sampled for lipid analyses at six time points during the experiment (Fig. 1c): days 0, 8, 19, 28, 56, and 83. At the start of the experiment (T0), 30 random tabs were collected from the holding tank before allocation to flow treatments. During the experiment, two to three tabs per raceway, per treatment, were sampled at each census, with all remaining tabs collected on day 83. At each time point, spat were carefully scraped from tabs using a sterile scalpel, transferred into 1 ml of filtered seawater in 1.5 ml Eppendorf tubes, and flash frozen at − 80°C for later lipid extraction.

## Tank husbandry

*Feeding regime* - Feeding was delivered daily (excluding weekends) using the same dosing-cone and peristaltic pump system as for symbiont inoculations. Each flume received a continuous 8 h feed at a constant pump rate of 10 ml $min^{-1}$ (4.8 l $day^{-1}$). Feeding was conducted during the dark phase of the light cycle, when coral polyps are generally most active (Houlbrèque and Ferrier-Pagès 2009). Feed consisted of mixed algae and rotifer suspension prepared fresh each morning (following Conlan et al.

2017). The algae mixture (*Isochrysis sp.*, *Rhodomonas sp.*, and *Tetraselmis sp.*) was supplied at a target concentration of ~ 2,000 cells $ml^{-1}$, while live rotifers (*Brachionus plicatilis*) were supplied at ~ 0.3 nauplii $ml^{-1}$. Because water throughput differed among flow regimes, the total volume of seawater passing through each flume during the 8 h feeding period increased from 288 l in the low flow treatment, to 1440 and 4320 l in the moderate, and high flow treatments, respectively. Feed concentrations in the dosing cones were therefore scaled in proportion to water throughput, so that target prey concentrations delivered to the flumes remained comparable despite the higher dilution and exchange rates in the moderate and high flow treatments. Consequently, dosing cones for higher-flow treatments contained more concentrated feed mixtures, with algal concentrations of approximately $1.2 \times 10^5$, $6.0 \times 10^5$, and $1.8 \times 10^6$ cells $ml^{-1}$ and rotifer concentrations of ~ 19, 93, and 279 nauplii $ml^{-1}$ for the low, moderate, and high flow treatments, respectively. Each cone was diluted to a final volume of 4.8 l using 4 µm-filtered seawater. After each feeding cycle, all cones and tubing were flushed with hot freshwater to minimise biofouling and prevent clogging of the peristaltic pump lines.

*Cleaning, light and temperature* - Tanks were cleaned twice weekly by siphoning detritus and gently brushing surfaces, PVC strips, and settlement tabs to remove turf algae. When spat were temporarily removed from the tanks for imaging, the flumes and raceways were scrubbed thoroughly. The light regime followed a 12 h light:12 h dark photoperiod on a reversed cycle (dark from 04:00–15:59; light from 16:00–03:59), with a 30-minute ramp-up and ramp-down. Maximum daily light intensity was 80 µmol photons $m^{-2}$ $s^{-1}$ (PAR). Water temperature was controlled via the SeaSim automated system and followed the reef-specific temperature profile for the experimental period (~ 27.5°C).

# Lipid extractions

Lipid samples, each consisting of all live spat scraped from a single tab, were freeze-dried for 48 h to remove residual moisture before lipid extraction using a FreeZone benchtop freeze dryer (Labconco, Kansas City, USA). Total lipids were extracted using dichloromethane:methanol (DCM:MeOH; 2:1, by volume) following a modified version of Folch et al. (1957). Samples were sonicated for 10 min to disrupt tissues, and the resulting extracts were filtered through cotton-packed glass Pasteur pipettes. The extraction was repeated twice, and all extracts were combined and washed with 0.44% potassium chloride (KCl) to remove contaminants before being left to settle overnight. The following morning, the lower (lipid-containing) layer was collected, and the solvent was evaporated under nitrogen at 35°C. Lipid content was then quantified gravimetrically using a four-decimal balance (AB 204; Mettler-Toledo, Greifensee, Switzerland). Following quantification, extracts were re-dissolved in DCM and stored at -20°C for lipid-class analysis. Owing to the low lipid content of coral spat, extracts were concentrated by evaporating 200 µl of DCM and re-dissolving the residue in 50 µl of DCM to achieve sufficient concentration for spotting.

Lipid class composition was determined using an Iatroscan MK 6s thin-layer chromatography-flame ionisation detector (Mitsubishi Chemical Medience, Tokyo, Japan) following Conlan et al. (2014). Each sample was spotted in duplicate onto silica-coated chromarods (5 µm particle size) with lipid separation

developed sequentially in polar (DCM:methanol:water, 50:20:2, by volume) and neutral (hexane:diethyl ether:formic acid, 60:15:1.5, by volume) solvents. Chromarods were dried at 100°C for 10 min prior to analysis. Peaks corresponding to major lipid classes were identified against analytical standards and quantified with the instrument software (PowerChrom version 2.5, eDAQ Pty Ltd). Lipid classes included wax and sterol esters (WE/SE), triacylglycerols (TAG), monoacylglycerols (MG), free fatty acids (FFA), sterols, phosphatidylserine/ phosphatidylethanolamine (PS/PE), phosphatidylcholine (PC), and lysophosphatidylcholine (LPC). Within the MG retention region, three peaks were detected, with only the first peak comparable in retention time to the MG standard. The second peak was consistently detected across samples but could not be assigned to a lipid class without an appropriate standard. The third peak was rare and made only a small contribution (Table S1). Sensitivity analyses showed that alternative pooling of these peaks did not change the main conclusion (Table S2). Hence, as a conservative approach, only the confirmed MG peak was included in functional interpretation and presented in figures. Lipid class data were expressed as the relative proportion of total lipid. Therefore, changes in lipid-class composition indicate shifts in relative lipid allocation rather than absolute increases or decreases in specific lipid pools. For interpretation, lipid classes were pooled into broad functional groups based on their primary biochemical roles: storage/reserve lipids included TAG and WE/SE; membrane-associated or structural lipids included PC, PS/PE, LPC, and sterols; and mobilisation/turnover lipids included MG and FFA (Imbs and Dembitsky 2023).

## Data analyses

All analyses were conducted in R version 4.5.2 (R Core Team 2025). Figures were generated in ‘ggplot2’ (Wickham 2016). Statistical significance was evaluated at $\alpha = 0.05$.

*Symbiont dosing method validation* – Pump outlet samples were analysed by pairing start- and end-of-day concentrations and comparing them within each flow regime using a linear mixed model with dosing batch as a random effect. Model significance was evaluated by analysis of variance (ANOVA). The response variable was log-transformed to quantify proportional change in concentration, and equivalence was visually assessed within ± 10%. Flume outlet samples were analysed separately to assess temporal changes in symbiont concentrations among flow regimes throughout the dosing and post-dosing phases. For each flume water sample, five technical replicate counts were performed on the flow cytometer and averaged to calculate symbiont concentration. Prior to analysis, unusually high or low technical counts within the same sample were identified using a modified z-score approach based on the median absolute deviation (Leys et al. 2013), which compares each technical count to the typical variation among replicate counts from the same sample. Flagged counts were manually inspected before exclusion (four counts from day 2 were excluded). Flume outlet samples were then analysed using a linear model with log-transformed cell concentrations as the response and flow × day as fixed effects. Model significance was evaluated by ANOVA, and estimated marginal means (± 95% CI) were back-transformed to the original scale (cells $ml^{-1}$) using the ‘emmeans’ package (Lenth 2025).

*Survival analysis* – Coral survival trajectories were compared among flow regimes using Kaplan–Meier (K-M) survival curves. Each coral was scored as alive or dead at each census, and individuals removed for lipid analyses were treated as right-censored at the time of extraction. Time was measured as days since settlement. Survival curves were fitted using the survfit function in the *survival* package (Therneau 2024) and visualised with *survminer* (Kassambara et al. 2025). Differences in survival among flow regimes were initially assessed using a log-rank test. A Cox proportional-hazards model was also fitted to estimate average hazard ratios among flow regimes, but the proportional-hazards assumption was violated (Schoenfeld $p < 0.001$; Grambsch and Therneau 1994). We therefore fitted a discrete-time hazard model with a binomial error distribution and complementary log–log link, including a flow × time interaction to allow treatment effects to vary through the experiment. Period-specific hazard ratios were then estimated for three time intervals: 0–35, 36–64, and 65–83 days. Pairwise comparisons among flow regimes were conducted within each interval, and the resulting hazard ratios were plotted per time period.

*Spat pigmentation score* – Spat pigmentation score was analysed using a cumulative link mixed model (CLMM) with a logit link and an ordered four-level response. Fixed effects included flow regime, time, and their interaction. Time was included as a continuous predictor and expressed in 10-day units to improve numerical scaling during model fitting (Harrison et al. 2018). This rescaling does not change the model structure, but means that time effects are interpreted per 10 days rather than per day. Random intercepts for raceway nested within flow regime and tab nested within raceway were included to account for the hierarchical structure of the experiment and repeated observations through time. The flow × time interaction was assessed by comparing the interaction model with an additive model without the interaction, using Akaike's Information Criterion (AIC) and a likelihood-ratio test. Post-hoc pairwise comparisons among flow regimes were conducted using estimated marginal means with Tukey adjustment when overall effects were significant.

*Lipid analyses* - Total lipid content was expressed as lipid content per spat by dividing the total lipid mass of each pooled sample by the number of spat in that sample. Baseline samples (T0) are shown descriptively only and were excluded from inferential models. Lipid content per spat was $\log_{10}$-transformed and analysed using a linear model with flow regime and sampling time as fixed, additive effects; the flow × sampling time interaction was tested but excluded because it was not significant. Model significance was assessed using ANOVA, with Tukey-adjusted estimated marginal means used for pairwise comparisons among flow regimes.

Lipid-class composition was analysed from the relative proportions of detected lipid classes. Baseline samples (T0) are again shown descriptively only and were excluded from inferential models. Overall differences in lipid-class composition were tested using PERMANOVA based on Bray–Curtis dissimilarities, with flow regime, experimental day, and their interaction as fixed effects. Homogeneity of multivariate dispersion was assessed for both flow regime and experimental day. To identify which lipid classes contributed to compositional differences, each class was analysed separately using linear models on arcsine-square-root-transformed proportions, with flow regime and experimental day as fixed

effects. P-values from class-specific tests were adjusted across lipid classes using the Benjamini-Hochberg false discovery rate procedure (Benjamini and Hochberg 1995). PS/PE was included in the overall lipid-class composition analysis but excluded from class-specific follow-up models because there were too few observations to fit reliable univariate models for this class. Lastly, lipid classes were also pooled into broad functional groups representing storage/reserve lipids (TAG and WE/SE), membrane-associated/structural lipids (PC, PS/PE, LPC), and mobilisation/turnover lipids (MG and FFA). Functional-group composition was calculated as the summed relative proportion of lipid classes within each group for each sample. Each functional group was analysed separately using linear models on arcsine-square-root-transformed proportions, with flow regime and experimental day as fixed effects. The flow × experimental day interaction was tested but excluded from the final models because it was not significant.

## Results

# Symbiont dosing method validation

Symbiont concentrations at the pump outlets were stable across days and flow regimes, with no difference between the start and end of daily dosing ($F_{2,22}$ = 1.19, $p$ = 0.32; Fig. 2a), indicating consistent and even delivery of symbiont cells during the dosing phase. Symbiont concentrations at the flume outlets were close to the target of 150 cells $ml^{-1}$ at the start of the dosing phase (Fig. 2b). From days 1–6, outlet concentrations averaged ~ 160–270 cells $mL^{-1}$ across flow regimes and did not differ significantly among flumes ($F_{2,42}$ = 0.75, $p$ = 0.48). Concentrations declined rapidly once dosing ceased after day 6, falling below 10 cells $ml^{-1}$ by day 9, indicating that symbiont cells did not remain in suspension for long. Overall, symbiont concentrations remained stable throughout the dosing period, confirming continuous and uniform delivery across all flow regimes.

# Survival

Survival differed significantly among flow regimes (Fig. 3a, log-rank $\chi^2$ = 27.2, df = 2, p < 0.001). Survival was lower under low flow than under moderate flow (pairwise log-rank test, p < 0.001) and high flow (p = 0.001), whereas moderate and high flow did not differ (p = 0.20). By the final census, survival estimates were lowest under low flow (0.47, 95% CI 0.41–0.55), highest under moderate flow (0.65, 95% CI 0.59–0.72), and intermediate under high flow (0.56, 95% CI 0.50–0.63). However, the effect of flow on mortality risk changed through time (Fig. 3b, flow × period LRT $\chi^2$ = 103.1, df = 4, p < 0.001). Early in the experiment (0–35 days), the mortality risk was 6.1-fold greater under low flow than under moderate flow (95% CI 3.2–11.6) and 21.7-fold greater under low flow than under high flow (95% CI 6.8–69.0), with no difference between moderate and high flow treatments. The same pattern persisted through 36–64 days, but by days 65–83 the effect reversed, with mortality risk lowest under low flow, intermediate under moderate flow, and highest under high flow (hazard ratio (HR) = 0.53 vs moderate; HR = 0.36 vs

high). This late reversal reduced differences among treatments by the final census, but cumulative survival remained lowest under low flow.

# Spat pigmentation score

Spat pigmentation score increased through time, but the pattern differed among flow regimes (Fig. 4; Tables S3, S4). The model including the flow × time interaction was better supported than the additive model (LRT $\chi^2$ = 11.34, df = 2, p = 0.003; ΔAIC = 7.34). Under low flow, pigmentation increased significantly through time (estimate = 0.915 ± 0.031 SE per 10 days, z = 29.51, p < 0.001), and pigmentation scores remained highest under low flow, intermediate under moderate flow (estimate = -2.413 ± 0.282 SE, z = -8.57, p < 0.001) and lowest under high flow (estimate = -3.281 ± 0.362 SE, z = -9.05, p < 0.001). The rate of increase was similar under low and moderate flow (interaction estimate = -0.060 ± 0.045 SE, z = -1.33, p = 0.183), but was slower under high flow than low flow (estimate = -0.200 ± 0.058 SE, z = -3.47, p < 0.001). Pairwise comparisons at days 19, 43, and 83 showed consistently that pigmentation scores were highest under low flow, intermediate under moderate flow, and lowest under high flow (all p ≤ 0.001; Table S3).

# Lipids

Total lipid content per spat differed significantly among flow treatments (Fig. 5a, $F_{2,38}$ = 17.92, p < 0.001) but did not vary through time ($F_{4,38}$ = 1.52, p = 0.217). Spat in the low-flow regime had higher lipid content than those in the moderate (p = 0.002) and high (p < 0.001) flow regimes, whereas lipid content did not differ significantly between the moderate and high flow regimes (p = 0.076).

In contrast, lipid-class composition differed significantly over time (Fig. 5b; PERMANOVA, $F_{4,29}$ = 5.58, $R^2$ = 0.362, p = 0.001) but not among flow treatments ($F_{2,29}$ = 0.73, $R^2$ = 0.024, p = 0.683) and there was no time × flow interaction ($F_{8,29}$ = 1.12, $R^2$ = 0.145, p = 0.324). Temporal shifts in the lipid composition were associated with changes in SE, TAG, LPC and sterols (all adjusted p ≤ 0.047). When lipid classes were pooled into functional groups, relative lipid allocation again changed through time but not among flow regimes (Fig. 5c). Storage/reserve lipids declined strongly over time ($F_{4,37}$ = 14.5, adjusted p < 0.001), while membrane/structural lipids changed modestly through time ($F_{4,37}$= 4.19, adjusted p = 0.013) and mobilisation/turnover lipids did not vary significantly over the same period ($F_{4,37}$ = 2.44, adjusted p = 0.127). Flow did not significantly affect any functional lipid group (all adjusted p ≥ 0.30).

## Discussion

Water flow had contrasting effects on early post-settlement performance in *Acropora digitifera*. Low flow promoted faster visible pigmentation development and higher total lipid content, but this did not translate into improved survival. Instead, cumulative survival remained lowest under low flow, largely because mortality risk was greatest under low flow during the early post-settlement period (up until 64

days). Moderate and high flow supported higher early survival despite lower pigmentation scores and lower lipid content, although mortality risk shifted later in the experiment (> 64 days) and became highest under high flow. This late reversal reduced differences among treatments by the final census, but did not fully offset the early mortality under low flow. These findings suggest that the hydrodynamic conditions favouring early symbiosis establishment and lipid accumulation are not necessarily the same as those that favour persistence through the early post-settlement bottleneck. Rather than identifying a single optimal flow regime, our findings indicate that hydrodynamic conditions shape coral spat performance through multiple, partly decoupled responses. These findings have implications for coral aquaculture and restoration, where flow conditions are often managed to improve settlement, growth and survival, but where improvements in one performance metric may not translate into higher overall recruitment success.

# Flow effects on early survival

The higher early mortality under low flow observed in our study is consistent with the expectation that reduced water movement can intensify boundary-layer limitation around coral tissues, restricting mass transfer, gas exchange and waste removal (Dennison and Barnes 1988; Hoogenboom and Connolly 2009). Low flow may also have affected spat indirectly by altering the surrounding benthic community. Even though tanks and tabs were cleaned regularly, lower water movement may have allowed microbial films, turf algae, or cyanobacteria to build up locally, intensifying competition, overgrowth, microbial interactions (Doropoulos et al. 2016; Jorissen et al. 2016). In contrast, higher flow conditions may reduce boundary-layer stagnation and limit the build-up of these benthic communities. This interpretation is broadly consistent with field-based coral-seeding work on the same species, where sexually propagated *A. digitifera* spat deployed on engineered seeding devices had higher survival at wave-exposed sites than at low-energy sites (Whitman et al. 2025). However, our results also complicate the idea that more flow is always better, as low flow promoted pigmentation and total lipid content among surviving spat, which could have longer term benefits that we were unable to follow here. It seems like flow affected different aspects of spat performance in different ways: the conditions that improved early survival were not the same as those associated with faster pigmentation development or larger lipid content. This response-specific pattern is consistent with other coral studies showing that flow can improve some outcomes but not others. For example, increased flow improved survival and growth in juvenile *Montipora capitata*, but no single combination of abiotic conditions maximised survival, growth, and bleaching tolerance (Hancock et al. 2021). Similarly, optimal flow conditions for prey capture in newly settled corals can differ among species and may not match the flow conditions that optimise other physiological functions (Geertsma et al. 2022). Together, these findings suggest that flow conditions that appear beneficial for one aspect of spat performance may come at a cost to other aspects of performance and therefore may not consistently maximise survival through the post-settlement bottleneck.

# Symbiont acquisition and survival

Early symbiont acquisition can enhance post-settlement survival in *Acropora* (Suzuki et al. 2013), but our results showed that faster visible pigmentation was not associated with higher survival. The treatment with the highest pigmentation scores also had the highest early mortality, suggesting that greater apparent symbiont acquisition was not sufficient to offset the survival costs associated with low flow. This supports the idea that the costs and benefits of symbiosis are context-dependent. For example, Chamberland et al. (2017) showed that larvae with higher maternally inherited symbiont densities were more vulnerable under thermal stress. The relationship between pigmentation and survival may also depend on which symbionts are acquired because different Symbiodiniaceae taxa can vary in their growth rates and the benefits they provide to the host, and nutrient exchange can depend on symbiont identity, density, and relative abundance (McIlroy et al. 2022). Thus, higher visible pigmentation may indicate greater symbiont presence, but not necessarily greater functional benefit. Rather than treating pigmentation as a simple indicator of improved condition, our results suggest that the consequences of symbiont acquisition depend on the hydrodynamic environment in which symbiosis develops.

# Lipid reserves and energetic condition

Lipid responses suggest that total lipid content alone does not fully capture the condition or survival potential of *A. digitifera* spat. Given the high energetic demands of settlement and early calcification, we expected lipid content to provide useful insight into spat condition. Yet, the higher lipid content under low flow did not correspond with higher survival, indicating that total lipid content was not sufficient on its own to predict survival through the early post-settlement bottleneck. Additionally, flow affected the total amount of lipid per spat but did not alter lipid-class composition, which instead shifted through time. This temporal shift was driven particularly by a decline in storage lipids as spat developed, suggesting that spat were progressively drawing on internal lipid reserves, potentially including maternally derived stores, during early development. Storage lipids such as triacylglycerols, wax esters, and sterol esters can support energetic demands associated with settlement, metamorphosis, tissue growth, and calcification, although they differ in turnover rate, with triacylglycerols generally considered more rapidly mobilised than wax and sterol esters (Harii et al. 2007; Figueiredo et al. 2012; Roper et al. 2024). The decline in these lipid classes is therefore consistent with energetic mobilisation during early post-settlement development (Figueiredo et al. 2012; Boulotte et al. 2023). At the same time, changes in structural lipids, including phospholipids and sterols, may reflect broader developmental changes associated with membrane organisation, cellular function, and the establishment of symbiosis (Roper et al. 2024; Matthews et al. 2025). However, whether these lipid shifts reflect normal developmental energy use, limited replenishment of lipid reserves, or differences in autotrophic and heterotrophic inputs remains difficult to resolve. Low flow may have increased the local retention and uptake of symbionts, which could have increased photosynthate supply to surviving spat. Early symbiont acquisition has been shown to reduce lipid consumption and improve larval survival and juvenile growth in *A. tenuis* (Hazraty-Kari et al. 2022). However, because spat were also fed throughout the experiment, the higher lipid content under low flow could also reflect greater retention of suspended food particles, increased prey encounter or capture, or selective survival of individuals that already had larger lipid reserves. Distinguishing among symbiont-derived energy, heterotrophic feeding, and selective survival is difficult

because coral lipid profiles can reflect both autotrophic and heterotrophic inputs, and are influenced by food availability, light, and environmental conditions (Conlan et al. 2020). Heterotrophic feeding can improve recruit performance, but lipid responses may be decoupled from survival and growth, as shown in *Acropora* recruits where feeding regimes affected performance while total lipids remained relatively stable and lipid-class responses were species-specific (Conlan et al. 2017). Therefore, lipid reserves provide useful physiological information, but they should not be treated as a stand-alone proxy for recruitment success.

# Mechanistic interpretation

A possible explanation for these contrasting responses is that low flow increased the residence time of suspended symbiont cells near the spat, potentially increasing opportunities for uptake, while also creating less favourable boundary-layer conditions for very small coral settlers. Reduced water exchange may have prolonged exposure to symbiont cells and contributed to faster visible pigmentation, but it may also have restricted gas exchange and waste removal, intensified oxygen and pH fluctuations near the tissue surface (Pacherres et al. 2020; Martins et al. 2024). Reduced water movement may also have promoted local fouling or microbial-film development around the tabs, further contributing to early mortality (Montalvo-Proano et al. 2025). These combined effects could explain why spat under low flow showed higher pigmentation and lipid content among survivors, yet experienced the greatest early mortality. If low flow promoted greater symbiont uptake or faster establishment, the benefits of increased photosynthate may have been offset by greater metabolic demand, stronger oxygen and pH fluctuations near the spat surface. This is consistent with evidence that high symbiont densities can increase vulnerability under stressful environmental conditions (Chamberland et al. 2017). The time-dependent survival patterns also support this idea: flow effects were strongest early in the experiment, but later weakened or reversed among the remaining spat, suggesting that the flow conditions that favour survival may shift as spat establish, acquire symbionts, and grow. Together, these patterns suggest a possible trade-off between early survival and survivor condition. Moderate and high flow supported higher early survival, whereas low flow produced fewer survivors with higher pigmentation scores and lipid content. Longer-term studies are needed to determine whether low-flow survivors gain a later advantage or whether the early survival benefits under moderate and high flow persist.

# Limitations and experimental context

Several limitations should be considered when interpreting these results. First, lipid analyses were based on pooled spat because individual spat did not provide sufficient biomass, reducing sample size and preventing direct links among individual survival, pigmentation, and lipid content. In addition, lipid-class composition was expressed as relative proportions, so temporal changes reflect shifts in lipid allocation rather than absolute changes in each lipid class. Future studies would benefit from larger experimental designs that provide enough biomass to measure absolute lipid-class concentrations, as well as from more sensitive lipidomic or metabolomic approaches, such as LC-MS/MS, which can resolve individual lipid compounds in corals (Reddy et al. 2023). Combined with stable isotope or tracer analyses these approaches could help determine whether lipid changes reflect use of internal reserves, replenishment

through autotrophic or heterotrophic inputs, or selective survival of individuals with higher energetic condition (Tremblay et al. 2015),.

Second, symbiont acquisition was assessed using a qualitative visual pigmentation score rather than direct cell counts or photosynthetic measurements. Although visual pigmentation can provide a useful relative indicator of symbiont-associated chlorophyll content in corals (Winters et al. 2009), it should not be interpreted as an absolute measure of symbiont density or photosynthetic performance. Furthermore, lipid and pigmentation responses could also be influenced by the experimental conditions and thus warrant caution in their interpretation. Spat were both fed and inoculated with symbionts using similar dosing systems, so higher lipid content under low flow cannot be attributed solely to symbiont-derived nutrition. It may also reflect differences in prey encounter, retention of suspended particles, or selective survival of better-provisioned spat. In addition, spat were inoculated with a single cultured symbiont strain, whereas naturally recruiting corals may encounter more diverse Symbiodiniaceae communities, with uptake shaped by both environmental availability and host selectivity (Quigley et al. 2017). Therefore, the relationship between pigmentation and survival observed here may differ under natural acquisition from mixed environmental sources. The experimental timeframe is also important. Had the experiment ended earlier, moderate and high flow would have appeared clearly favourable for survival; had it continued longer, the later increase in mortality under high flow may have further altered treatment rankings. Longer-term studies that follow spat toward size-escape thresholds are needed to determine whether early differences in survival, pigmentation, and lipid reserves translate into lasting recruitment benefits. Finally, because this study focused on a single species from one spawning cohort, broader generalisations about coral spat responses to flow should be made cautiously, particularly because settlement behaviour and post-settlement survival can vary strongly among coral species and reproductive strategies (Ritson-Williams et al. 2016). Repeating this experiment with greater tank-level replication, multiple species, and longer monitoring would help determine whether the early mortality under low flow represents a persistent disadvantage, or whether surviving low-flow spat remain stable and eventually outperform spat reared under moderate or high flow.

# Implications for coral aquaculture and restoration

Our findings highlight that flow conditions can shape early post-settlement coral performance in complex ways. Flow is often managed in aquaculture to support settlement, growth, and survival, but our results suggest that these outcomes may not respond uniformly. A flow regime associated with faster visible symbiont acquisition or higher lipid reserves may not necessarily maximise early survival, and the most suitable conditions may change through development. Rather than providing a direct recommendation for rearing conditions, our study highlights the need for future work that assesses multiple performance metrics across longer timeframes, with greater replication and a broader range of coral species. This will help determine whether post-settlement rearing conditions should be tailored to specific processes or developmental stages, rather than applying a single flow condition throughout early rearing. This is consistent with other studies on early post-settlement coral performance showing that optimal conditions can differ among species, processes, and response variables (Forsman et al.

2012; Hancock et al. 2021; Geertsma et al. 2022), and with field-based evidence that hydrodynamic and reef-zone context can strongly shape natural recruitment patterns and seeded-coral survival (Drake et al. 2025; Whitman et al. 2025), often in species-, method-, and scale-dependent ways (Jurriaans et al. 2025, 2026). As coral restoration increasingly relies on sexually propagated corals to increase genetic diversity and scale interventions (Randall et al. 2020, Banaszak et al. 2023), improving understanding of early post-settlement bottlenecks will be critical for developing more effective coral-seeding approaches.

# Declarations

**Author contributions:**

SJ, CAS and CJR conceived and designed the study, SJ and CAS conducted the experiment. SJ, MD, AW and VJ conducted laboratory and image analyses. SJ analysed the data and wrote the manuscript with input from all authors.

**Acknowledgements**

We acknowledge the Gunggandji, Bindal, and Wulgurukaba Peoples as the Traditional Custodians of the land and sea Countries where this research took place and pay our respects to Elders past, present and emerging. We thank them for providing Free Prior Informed Consent to undertake this work. Coral collections were conducted under Reef Authority permit G21/45348.1. Funding was provided by the Reef Restoration and Adaptation Program (RRAP), a partnership between the Australian Government's Reef Trust and the Great Barrier Reef Foundation. We thank the National Sea Simulator staff and Maren Toor for their expertise and assistance with this experiment. We are especially grateful to Phil Mercurio for his extensive support and expertise in lipidomics, which greatly contributed to this study.

Funding was provided by the Reef Restoration and Adaptation Program (RRAP), a partnership between the Australian Government's Reef Trust and the Great Barrier Reef Foundation.

The authors declare no competing interests.

Data are available through AIMS data repository (link to be provided upon acceptance DOI XXXX). Scripts are available via GitHub (SaskiaJurriaans/FlowExp).

# References

1. Atkinson M, Bilger R (1992) Effects of water velocity on phosphate uptake in coral reef-hat communities. Limnology and Oceanography 37:273–279
2. Baird AH, Guest JR, Willis BL (2009) Systematic and biogeographical patterns in the reproductive biology of scleractinian corals. Annual review of ecology, evolution, and systematics 40:551–571
3. Banaszak AT, Marhaver KL, Miller MW, Hartmann AC, Albright R, Hagedorn M, Harrison PL, Latijnhouwers KR, Mendoza Quiroz S, Pizarro V (2023) Applying coral breeding to reef restoration:

best practices, knowledge gaps, and priority actions in a rapidly-evolving field. Restoration Ecology 31:e13913

4. Benjamini Y, Hochberg Y (1995) Controlling the false discovery rate: a practical and powerful approach to multiple testing. Journal of the Royal statistical society: series B (Methodological) 57:289–300
5. Boulotte NM, Rudd D, Harrison PL, Humphrey C, Benkendorff K (2023) Nanodelivery of lipids to coral larvae maximises post-settlement survival: Implications for larval ecology and reef restoration.
6. Briggs ND, Page CA, Giuliano C, Alessi C, Hoogenboom M, Bay LK, Randall CJ (2024) Dissecting coral recovery: bleaching reduces reproductive output in Acropora millepora. Coral Reefs 43:557–569
7. Chamberland VF, Latijnhouwers KR, Huisman J, Hartmann AC, Vermeij MJ (2017) Costs and benefits of maternally inherited algal symbionts in coral larvae. Proceedings of the Royal Society B: Biological Sciences 284:
8. Conlan J, Bay L, Jones A, Thompson A, Francis D (2020) Seasonal variation in the lipid profile of Acropora millepora at Halfway Island, Great Barrier Reef. Coral Reefs 39:1753–1765
9. Conlan JA, Humphrey CA, Severati A, Francis DS (2017) Influence of different feeding regimes on the survival, growth, and biochemical composition of Acropora coral recruits. PloS one 12:e0188568
10. Conlan JA, Jones PL, Turchini GM, Hall MR, Francis DS (2014) Changes in the nutritional composition of captive early-mid stage Panulirus ornatus phyllosoma over ecdysis and larval development. Aquaculture 434:159–170
11. Dennison WC, Barnes DJ (1988) Effect of water motion on coral photosynthesis and calcification. Journal of Experimental Marine Biology and Ecology 115:67–77
12. Doropoulos C, Roff G, Bozec Y-M, Zupan M, Werminghausen J, Mumby PJ (2016) Characterizing the ecological trade-offs throughout the early ontogeny of coral recruitment. Ecological Monographs 86:20–44
13. Drake MA, Noonan SH, Alvarez-Noriega M, Rashid AR, Fabricius KE (2025) Current velocity, water quality, and benthic taxa as predictors for coral recruitment rates on the Great Barrier Reef. PloS one 20:e0319521
14. Duckworth A, Giofre N, Jones R (2017) Coral morphology and sedimentation. Marine Pollution Bulletin 125:289–300
15. Eagle JV, Baird AH, Jones GP, Kingsford MJ (2012) Recruitment hotspots: consistent spatial patterns in the relative abundance of coral recruits at One Tree Island, Australia. Galaxea, Journal of Coral Reef Studies 14:5–22
16. Eakin CM, Heron SF, Connolly SR, Devotta DA, Liu G, Geiger EF, De La Cour JL, Gomez AM, Skirving WJ, Baird AH, Cantin NE, Couch CS, Donner SD, Gilmour J, Gonzalez-Rivero M, Gudka M, Harrison HB, Hodgson G, Hoegh-Guldberg O, Hoey AS, Hoogenboom MO, Hughes TP, Johnson ME, Kerry JT, Kimura T, Mihaly J, Muñiz-Castillo AI, Obura DO, Pratchett MS, Rivera-Sosa A, Ross CL, Stein J, Thompson A, Torda G, Viehman TS, Walter CS, Wilson S, Marsh BL, Spady BL, Dyer N, Adam TC,

Alcolado P, Alidoostsalimi M, Alidoostsalimi P, Alvarez-Filip L, Álvarez-Noriega M, Arias-González JE, Bahr KD, Barnes P, Barraza Sandoval JE, Baum JK, Bauman AG, Beger M, Berry K, Bessell-Browne P, Bigot L, Bonito V, Brodnicke OB, Burdick D, Burkepile DE, Burt AJ, Burt JA, Butler IR, Caldwell JM, Chancerelle Y, Chen CA, Cherh K-L, Childress MJ, Coker DJ, Costa B, Coward G, Crabbe MJC, Dallison T, Dalton S, DeCarlo TM, Drury C, Drysdale I, Edwards CB, Eggertsen L, Elma E, Ennis RS, Evans RD, Eyal G, Fenner D, Figueroa-Zavala B, Fisch J, Fox MD, Gadoutsis E, Gilbert A, Halford AR, Heintz T, Hewlett J, Hobbs J-PA, Hoot WC, Houk P, Johnston L, Johnston MA, Kayanne H, Kennedy EV, Kikuchi RKP de, Kloiber U, Koike H, Kramer KL, Kuo C-Y, Lang J, Lawrence A, Leadbeater A, Leão ZMAN, Lee JN, Lewis C, Lirman D, Longo GO, MacDonald C, Mallela J, Mangubhai S, da Silva IM, Mason-Parker C, McDonough V, McField M, Mello T, Miternique-Agathe C, Madi M, Moldzio S, Monroe AA, Montefalcone M, Moses KS, Mostafavi PG, Moura RL de, Munasinghe CS, Mwaura J, Nakamura T, Nicet J-B, Nuttall MF, Oliveira MDM, Oxenford HA, Pandolfi JM, Patankar V, Perez D, Perera N, Prabuning D, Precht W, Raj KD, Reimer JD, Richardson LE, Rotjan R, Ryan N, Salm R, Sandin SA, Schopmeyer S, Shedrawi G, Shokri MR, Smith JE, Smith K, Smith SR, Smith TB, Sommer B, Soto M, Suckoo R, Sykes H, Tagarino KA, Teoh M, Thai MQ, Toh TC, Tredinnick A, Tso A, Tyley H, Ussi AM, Vargas-Angel B, Vaterlaus C, Vermeij MJA, Vo ST, Voolstra CR, Wee HB, Weiler BA, Williams DE, Yahya SAS, Yeemin T, Ziegler M, Manzello DP (2026) Severe and widespread coral reef damage during the 2014–2017 Global Coral Bleaching Event. Nature Communications 17:1318

17. Edmunds PJ (2023) Coral recruitment: patterns and processes determining the dynamics of coral populations. Biological Reviews 98:1862–1886
18. Edmunds PJ, Cumbo VR, Fan T-Y (2013) Metabolic costs of larval settlement and metamorphosis in the coral Seriatopora caliendrum under ambient and elevated pCO2. Journal of Experimental Marine Biology and Ecology 443:33–38
19. Emslie MJ, Ceccarelli DM, Logan M, Blandford MI, Bray P, Campili AR, Cantin N, Choukroun S, Cole A, Jonker MJ (2025) Anthropogenic climate change causes substantial loss of coral on the northern Great Barrier Reef during the 2024 bleaching event. Coral Reefs 1–17
20. Ferrara EF, Bauer L, Puntin G, Bautz F, Celayir S, Do M, Eck F, Heider M, Wissel P, Arnold A (2026) Red, green, blue color indices as proxy for Symbiodiniaceae cell density and chlorophyll content during coral bleaching. Limnology and Oceanography: Methods e70047
21. Figueiredo J, Baird AH, Cohen MF, Flot J-F, Kamiki T, Meziane T, Tsuchiya M, Yamasaki H (2012) Ontogenetic change in the lipid and fatty acid composition of scleractinian coral larvae. Coral Reefs 31:613–619
22. Finelli CM, Helmuth BST, Pentcheff ND, Wethey DS (2006) Water flow influences oxygen transport and photosynthetic efficiency in corals. Coral Reefs 25:47–57
23. Folch J, Lees M, Stanley GS (1957) A simple method for the isolation and purification of total lipides from animal tissues. Journal of biological chemistry 226:497–509
24. Forsman ZH, Kimokeo BK, Bird CE, Hunter CL, Toonen RJ (2012) Coral farming: effects of light, water motion and artificial foods. Journal of the Marine Biological Association of the United Kingdom 92:721–729

25. Geertsma RC, Wijgerde T, Latijnhouwers KR, Chamberland VF (2022) Onset of zooplanktivory and optimal water flow rates for prey capture in newly settled polyps of ten Caribbean coral species. Coral Reefs 41:1651–1664
26. Gouezo M, Langlais C, Beardsley J, Roff G, Harrison PL, Thomson DP, Doropoulos C (2025) Going with the flow: Leveraging reef-scale hydrodynamics for upscaling larval-based restoration. Ecological Applications 35:e70020
27. Grambsch PM, Therneau TM (1994) Proportional hazards tests and diagnostics based on weighted residuals. Biometrika 81:515–526
28. Hancock JR, Barrows AR, Roome TC, Huffmyer AS, Matsuda SB, Munk NJ, Rahnke SA, Drury C (2021) Coral husbandry for ocean futures: leveraging abiotic factors to increase survivorship, growth, and resilience in juvenile Montipora capitata. Marine Ecology Progress Series 657:123–133
29. Harii S, Nadaoka K, Yamamoto M, Iwao K (2007) Temporal changes in settlement, lipid content and lipid composition of larvae of the spawning hermatypic coral Acropora tenuis. Mar Ecol Prog Ser 346:89–96
30. Harrison XA, Donaldson L, Correa-Cano ME, Evans J, Fisher DN, Goodwin CE, Robinson BS, Hodgson DJ, Inger R (2018) A brief introduction to mixed effects modelling and multi-model inference in ecology. PeerJ 6:e4794
31. Hazraty-Kari S, Masaya M, Kawachi M, Harii S (2022) The early acquisition of symbiotic algae benefits larval survival and juvenile growth in the coral Acropora tenuis. Journal of Experimental Zoology Part A: Ecological and Integrative Physiology 337:559–565
32. Heyward A, Negri A (1999) Natural inducers for coral larval metamorphosis. Coral reefs 18:273–279
33. Hoogenboom MO, Connolly SR (2009) Defining fundamental niche dimensions of corals: synergistic effects of colony size, light, and flow. Ecology 90:767–780
34. Houlbrèque F, Ferrier-Pagès C (2009) Heterotrophy in tropical scleractinian corals. Biological Reviews 84:1–17
35. Hughes TP, Kerry JT, Baird AH, Connolly SR, Chase TJ, Dietzel A, Hill T, Hoey AS, Hoogenboom MO, Jacobson M, Kerswell A, Madin JS, Mieog A, Paley AS, Pratchett MS, Torda G, Woods RM (2019) Global warming impairs stock–recruitment dynamics of corals. Nature 568:387–390
36. Humanes A, Fink A, Willis BL, Fabricius KE, de Beer D, Negri AP (2017) Effects of suspended sediments and nutrient enrichment on juvenile corals. Marine Pollution Bulletin 125:166–175
37. Illing B, Severati A, Hochen J, Boyd P, Raison P, Mather R, Downie AT, Rummer JL, Kroon FJ, Humphrey C (2021) Automated flow control of a multi-lane swimming chamber for small fishes indicates species-specific sensitivity to experimental protocols. Conservation physiology 9:coaa131
38. Imbs AB, Dembitsky VM (2023) Coral lipids. Marine Drugs 21:539
39. Jokiel PL (1978) Effects of water motion on reef corals. Journal of Experimental Marine Biology and Ecology 35:87–97

40. Jokiel PL, Morrissey JI (1993) Water motion on coral reefs: evaluation of the'clod card'technique. Marine Ecology Progress Series 93:175–181
41. Jorissen H, Skinner C, Osinga R, de Beer D, Nugues MM (2016) Evidence for water-mediated mechanisms in coral–algal interactions. Proceedings of the Royal Society B: Biological Sciences 283:20161137
42. Jurriaans S, Lefèvre CD, Allen K, Giuliano C, Page CA, Puotinen M, Radford B, Sims CA, Whitman TN, Randall CJ (2025) Wave energy and other environmental drivers as predictors of seeded-coral performance on the great barrier reef. Scientific Reports 15:38335
43. Jurriaans S, Lefèvre CD, Ferguson S, Randall CJ (2026) Propagation method and species drive survival patterns across reef zones in coral seeding on the Great Barrier Reef. Restoration Ecology e70358
44. Kassambara A, Kosinski M, Biecek P (2025) survminer: Drawing Survival Curves using "ggplot2."
45. Lenth RV (2025) Package 'emmeans.'
46. Lentz ME, Freel EB, Forsman ZH, Schar DWH, Toonen RJ (2024) Flow rates alter the outcome of coral bleaching and growth experiments. Discover Oceans 1:31
47. Leys C, Ley C, Klein O, Bernard P, Licata L (2013) Detecting outliers: Do not use standard deviation around the mean, use absolute deviation around the median. Journal of experimental social psychology 49:764–766
48. Lowe RJ, Falter JL, Monismith SG, Atkinson MJ (2009) A numerical study of circulation in a coastal reef-lagoon system. Journal of Geophysical Research: Oceans 114:
49. Madin JS, Black KP, Connolly SR (2006) Scaling water motion on coral reefs: from regional to organismal scales. Coral Reefs 25:635–644
50. Martins CPP, Ziegler M, Schubert P, Wilke T, Wall M (2024) Effects of water flow and ocean acidification on oxygen and pH gradients in coral boundary layer. Scientific Reports 14:12757
51. Matthews JL, Bartels N, Kish H, La Motta L, Padula MP, Hughes DJ, Crane ZJ, Humphrey C, Boulotte N, Roper C, Van Oppen MJH, Raina J-B, Suggett DJ (2025) Sterols are key to coral larvae survival, swimming capacity, and thermal tolerance. Commun Biol 8:1494
52. McIlroy SE, TerHorst CP, Teece M, Coffroth MA (2022) Nutrient dynamics in coral symbiosis depend on both the relative and absolute abundance of Symbiodiniaceae species. Microbiome 10:192
53. Montalvo-Proano J, Alvarez-Noriega M, Flores F, Severati A, Negri AP (2025) Fouling-release coatings enhance Acropora loripes coral spat survival by limiting algal competition on seeding devices. Frontiers in Marine Science 12:1684011
54. Nakamura T (2010) Importance of water-flow on the physiological responses of reef-building corals. Galaxea, Journal of Coral Reef Studies 12:1–14
55. Nakamura T v, Van Woesik R (2001) Water-flow rates and passive diffusion partially explain differential survival of corals during the 1998 bleaching event. Marine Ecology Progress Series 212:301–304

56. Pacherres CO, Ahmerkamp S, Schmidt-Grieb GM, Holtappels M, Richter C (2020) Ciliary vortex flows and oxygen dynamics in the coral boundary layer. Scientific reports 10:7541
57. Pollock FJ, Katz SM, van de Water JA, Davies SW, Hein M, Torda G, Matz MV, Beltran VH, Buerger P, Puill-Stephan E (2017) Coral larvae for restoration and research: a large-scale method for rearing Acropora millepora larvae, inducing settlement, and establishing symbiosis. PeerJ 5:e3732
58. Quigley KM, Bay LK, Willis BL (2017) Temperature and water quality-related patterns in sediment-associated Symbiodinium communities impact symbiont uptake and fitness of juveniles in the genus Acropora. Frontiers in Marine Science 4:401
59. R Core Team (2025) R: A Language and Environment for Statistical Computing.
60. Ramsby BD, Forster R, Ferguson SN, Haikola P, Randall CJ, Abdul Wahab MA, Mead DJ, Severati A (2025) Developing coral seeding devices and rapid deployment methods to scale up reef restoration. Restoration Ecology e70206
61. Randall C, Negri AP, Quigley KM, Foster T, Ricardo GF, Webster NS, Bay LK, Harrison PL, Babcock RC, Heyward AJ (2020) Sexual production of corals for reef restoration in the Anthropocene. Mar Ecol Prog Ser 635:203–232
62. Reddy MM, Goossens C, Zhou Y, Chaib S, Raviglione D, Nicolè F, Hume BC, Forcioli D, Agostini S, Boissin E (2023) Multi-omics determination of metabolome diversity in natural coral populations in the Pacific Ocean. Communications Earth & Environment 4:281
63. Reidenbach MA, Koseff JR, Koehl M (2009) Hydrodynamic forces on larvae affect their settlement on coral reefs in turbulent, wave-driven flow. Limnology and oceanography 54:318–330
64. Ritson-Williams R, Arnold SN, Paul VJ (2016) Patterns of larval settlement preferences and post–settlement survival for seven Caribbean corals. Marine Ecology Progress Series 548:127–138
65. Roper CD, Matthews JL, Camp EF, Padula MP, Kuzhiumparambil U, Edmondson J, Howlett L, Suggett DJ (2024) Lipid composition of coral propagules and reproductive material in coral restoration nurseries. Coral Reefs 43:1483–1496
66. Schneider CA, Rasband WS, Eliceiri KW (2012) NIH Image to ImageJ: 25 years of image analysis. Nature Methods 9:671–675
67. Siebeck U, Marshall N, Klüter A, Hoegh-Guldberg O (2006) Monitoring coral bleaching using a colour reference card. Coral Reefs 25:453–460
68. Smith HA, Dallmeyer-Drennen G, Bourne DG, Egan S, Page CA (2025) Sea-weeding enhances early coral survival on seeding devices, but benefits of seeding diminish after one year. Journal of Environmental Management 383:125322
69. Suzuki G, Yamashita H, Kai S, Hayashibara T, Suzuki K, Iehisa Y, Okada W, Ando W, Komori T (2013) Early uptake of specific symbionts enhances the post-settlement survival of Acropora corals. Marine Ecology Progress Series 494:149–158
70. Therneau TM (2024) A Package for Survival Analysis in R.

71. Trapon M, Pratchett M, Hoey A, Baird A (2013) Influence of fish grazing and sedimentation on the early post-settlement survival of the tabular coral Acropora cytherea. Coral Reefs 32:1051–1059
72. Tremblay P, Maguer JF, Grover R, Ferrier-Pages C (2015) Trophic dynamics of scleractinian corals: stable isotope evidence. The Journal of experimental biology 218:1223–1234
73. Whitman TN, Jurriaans S, Lefevre C, Sims CA, Radford B, Puotinen M, Hoogenboom MO, Negri AP, Randall CJ (2025) Seeded Acropora digitifera corals survive best on wave-exposed reefs with grazing from small fishes. Restoration Ecology e70016
74. Wickham H (2016) ggplot2: Elegant Graphics for Data Analysis. Springer-Verlag New York,
75. Winters G, Holzman R, Blekhman A, Beer S, Loya Y (2009) Photographic assessment of coral chlorophyll contents: Implications for ecophysiological studies and coral monitoring. Journal of Experimental Marine Biology and Ecology 380:25–35

# Figures

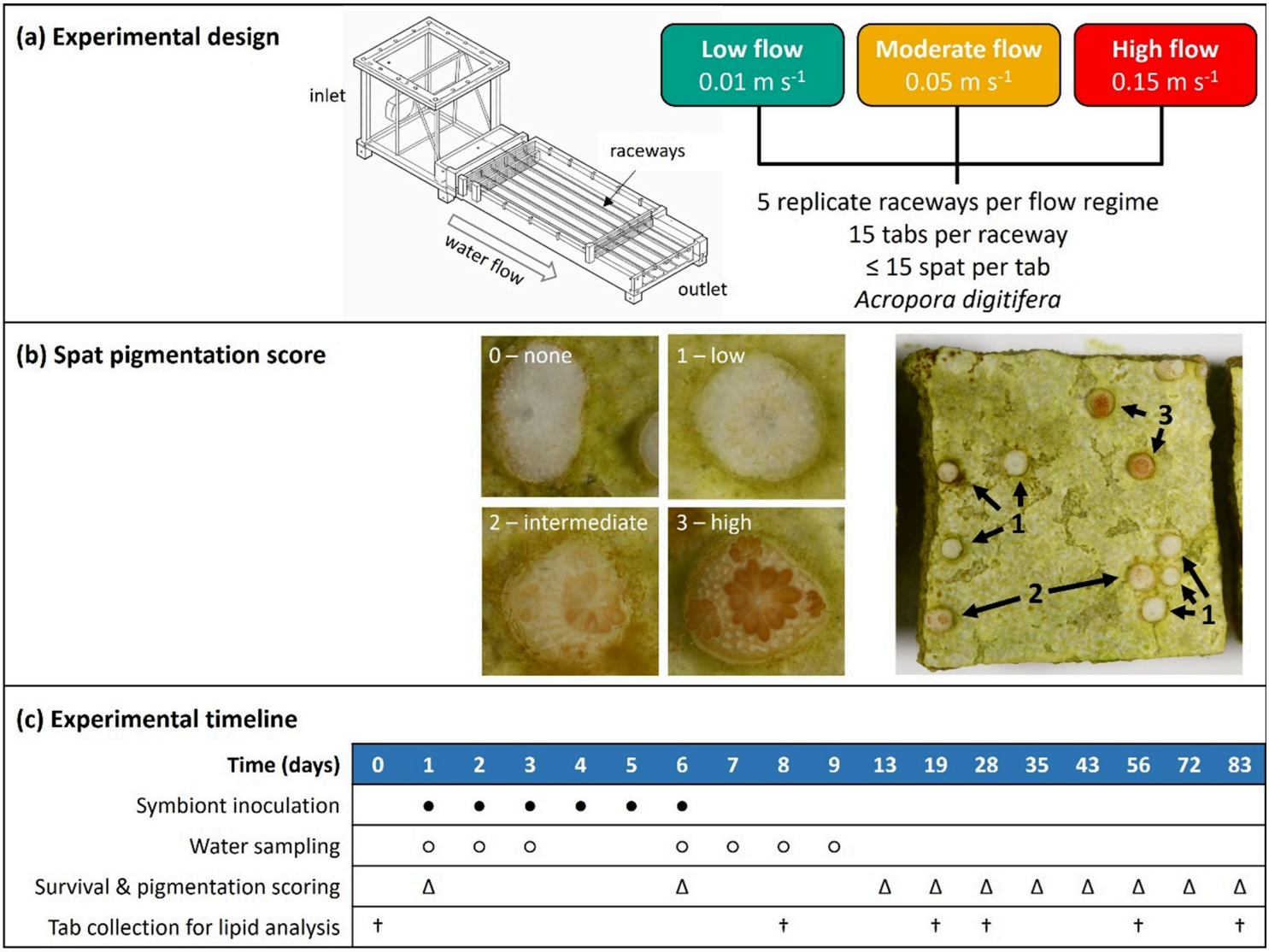



**Figure 1**

Experimental design, spat pigmentation scoring, and experimental timeline. (a) Three flume tanks were used to generate low, moderate, and high flow regimes. Each flow treatment included five replicate raceways with 15 tabs per raceway and up to 15 *Acropora digitifera* spat per tab. (b) Four-point visual scoring system used to assess spat pigmentation: 0 = none, 1 = low, 2 = intermediate, and 3 = high pigmentation. The right-hand image shows an example tab with spat assigned different pigmentation scores. (c) Experimental timeline showing symbiont inoculation days 1-6, water sampling days 1–9, repeated survival and spat pigmentation assessment days 1-83, and tab collections for lipid analyses days 0-83.

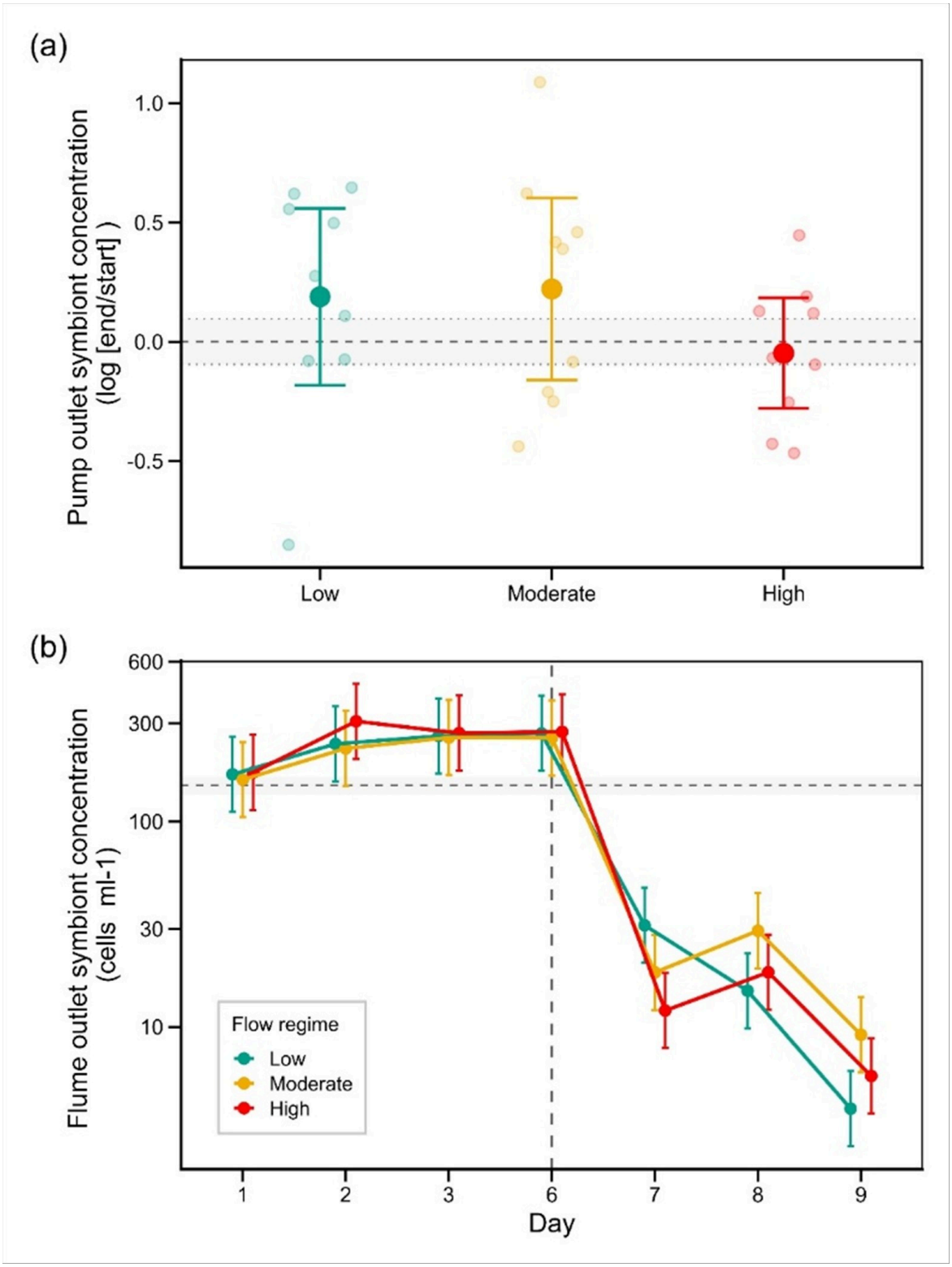



**Figure 2**

Validation of the symbiont dosing method for inoculation of coral spat. (**a**) Pump outlet concentrations expressed as log(end/start) over the daily dosing period for each flow regime. The dashed and dotted horizontal lines indicate no change between start and end of the dosing period and ±10% equivalence, respectively. Points and error bars represent mean ± 95% CI for each flow regime. (**b**) Symbiont concentrations measured at the flume outlets during the dosing phase (days 1–6) and post-dosing

phase (days 7–9). Points and error bars represent model-based means ± 95% CI. The horizontal dashed line indicates the target concentration (150 cells ml⁻¹), and the vertical dashed line indicates the end of dosing after day 6.

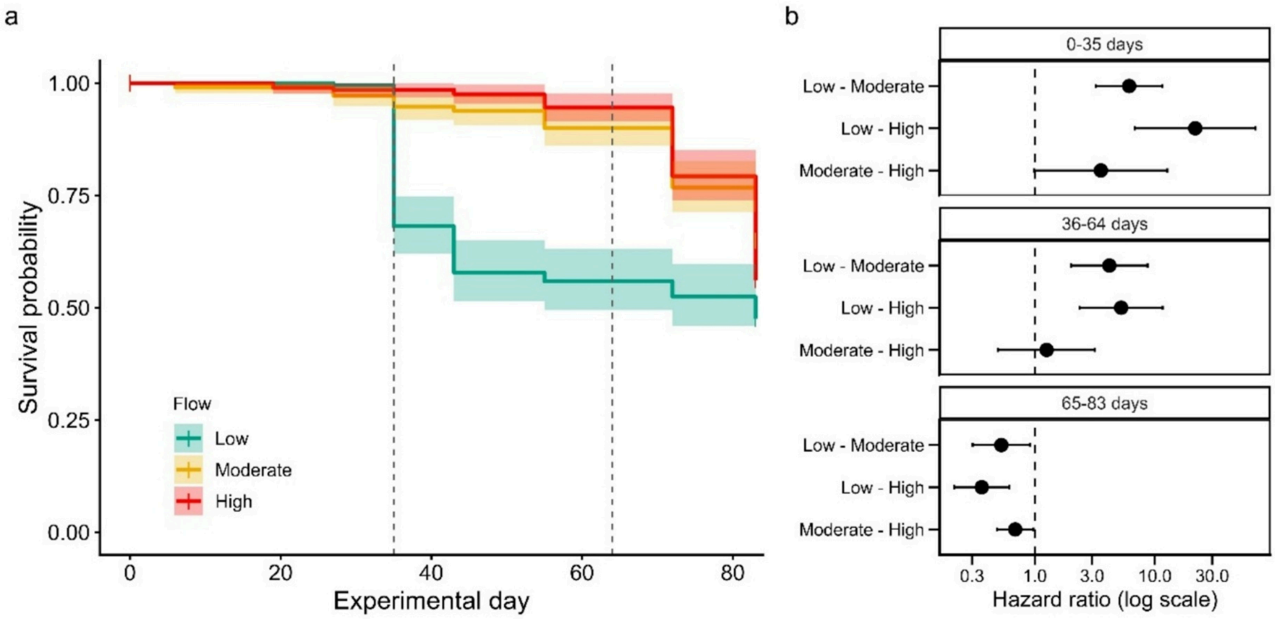



**Figure 3**

Flow-dependent survival and mortality risk of *Acropora digitifera* spat. (**a**) Kaplan–Meier survival curves (±95 % CI) under low (0.01 m $s^{-1}$), moderate (0.05 m $s^{-1}$), and high (0.15 m $s^{-1}$) flow. Vertical dashed lines indicate the time intervals used for the period-specific hazard-ratio (HR) estimates. (b) Period-specific hazard ratios (±95% CI, log scale) from a discrete-time hazard model showing pairwise comparisons among flow treatments. The dashed line indicates equal hazard (HR = 1), while values above 1 indicate higher mortality risk for the first flow treatment in each comparison, and values below 1 indicate lower mortality risk.

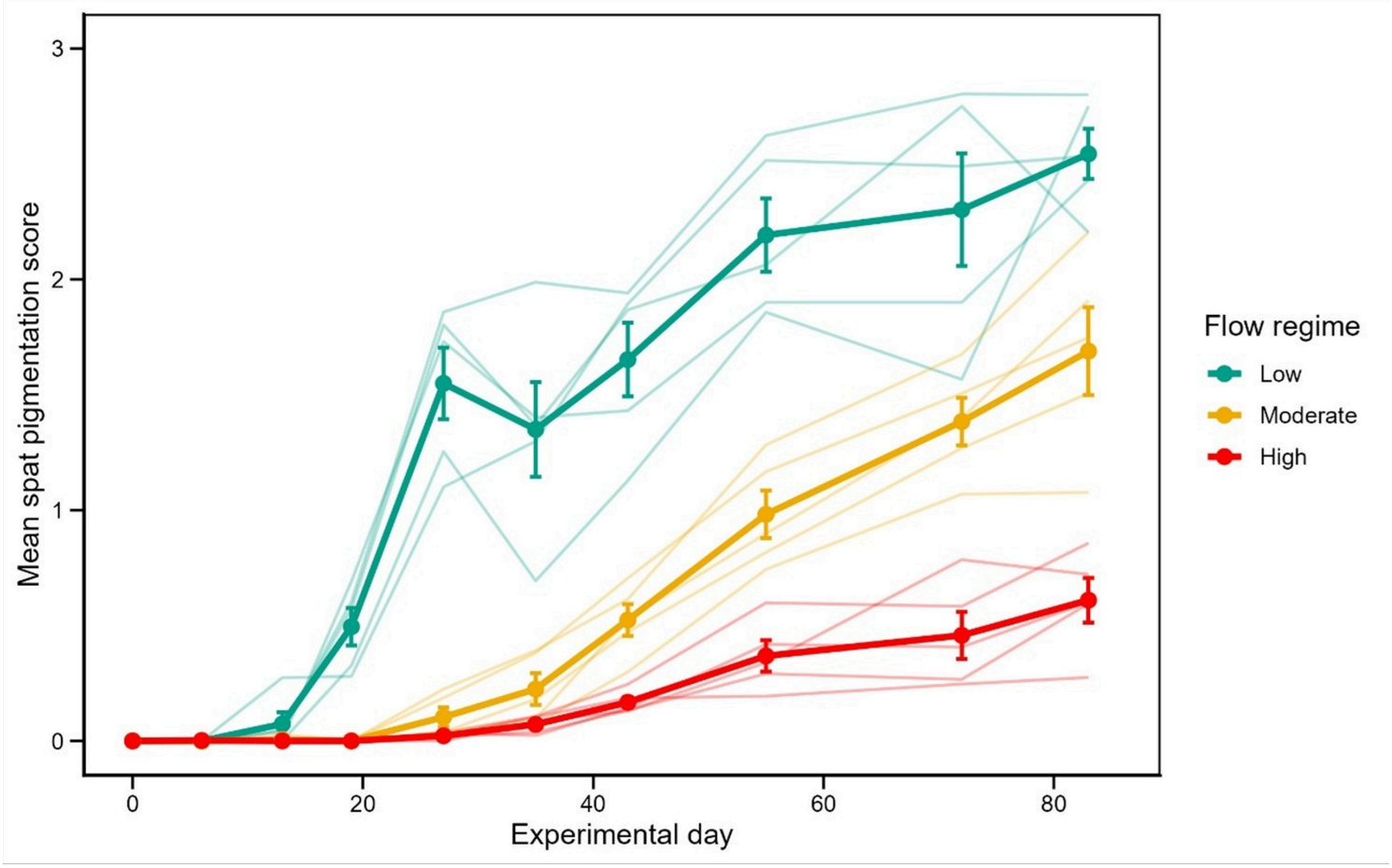



**Figure 4**

Mean pigmentation score of *Acropora digitifera* spat through time under low, moderate, and high flow regimes. Thin transparent lines show raceway-level mean scores for each flow regime, and bold lines show treatment-level means across raceways. Error bars indicate ± SE around treatment-level means, calculated among raceways within each flow regime.

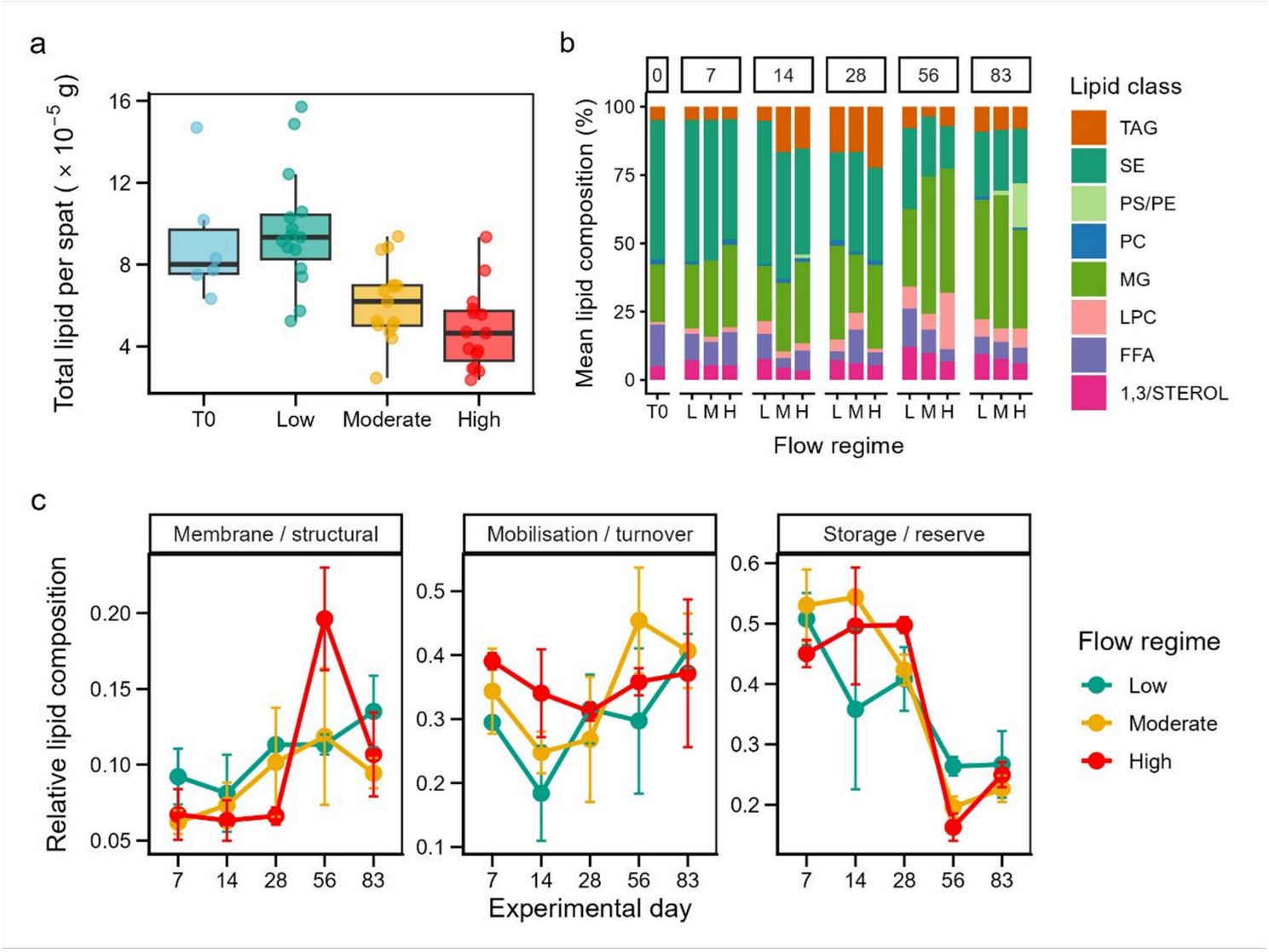



**Figure 5**

Total lipid content, lipid-class composition and functional group composition of *Acropora digitifera*spat. **(a)** Total lipid content per spat at the start of the experiment (T0) and under low, moderate, and high flow treatments, pooled across experimental days. Points represent individual samples. T0 samples represent the shared pre-treatment baseline and were excluded from inferential analyses.**(b)** Mean lipid-class composition (%) of spat over time within each flow treatment. Lipid classes are shown as proportions of total detected lipids for each flow × time combination. Numbers above the bars indicate sampling day. T0 represents the start of the experiment, and L, M, and H represent low, moderate, and high flow treatments, respectively. TAG = triacylglycerols; SE = sterol esters; MG = monoacylglycerols; LPC = lysophosphatidylcholine; FFA = free fatty acids; PC = phosphatidylcholine; PS/PE = phosphatidylserine/phosphatidylethanolamine; 1,3/STEROL = 1,3-diacylglycerols/sterols; (c) Relative lipid composition pooled into broad functional groups. Points show mean relative composition for each flow × time combination, and error bars indicate ± SE.

# Supplementary Files

This is a list of supplementary files associated with this preprint. Click to download.

- JurriaansetalFlowExpSupplement.docx